Synthesis and characterisation of magnetic-fluorescent Fe_3O_4@SiO_2@ZnS nanocomposites

Caidi Jiang, Zunli Mo, Bin Pu, Chun Zhang

College of Chemistry and Chemical Engineering, Northwest Normal University, Lanzhou 730070, People's Republic of China
E-mail: mozlnwnu2011@163.com

Published in Micro & Nano Letters; Received on 31st October 2013; Revised on 10th January 2014; Accepted on 28th January 2014

Bifunctional magnetic-fluorescent Fe_3O_4@SiO_2@ZnS nanocomposites were synthesised by a chemical deposition method. The Fe_3O_4 magnetic nanoparticles as the core were obtained by means of a solvothermal reaction with SiO_2 as the shell. ZnS particles were linked to Fe_3O_4@SiO_2 core–shell nanostructures. The morphology and properties of the resultant Fe_3O_4@SiO_2@ZnS nanocomposites were investigated by X-ray diffraction, field emission scanning electron microscopy, high-resolution transmission electron microscopy, a vibration sample magnetometer and fluorescence microscopy. The results showed that bead-like structures were built from numerous Fe_3O_4@SiO_2@ZnS microspheres with an average size of 250 nm. The saturation magnetisation (M_s) value of Fe_3O_4@SiO_2@ZnS nanocomposites was 22.41 emu/g at room temperature. Furthermore, a strong blue light emission was observed from the nanocomposites under UV light irradiation. The combination of magnetic and fluorescent properties may lead to Fe_3O_4@SiO_2@ZnS nanocomposites having a variety of potential applications in the field of biomedicine, such as bioimaging and cell separation.

1. Introduction: Magnetic-fluorescent nanocomposites with integrated functionalities have attracted increasing interest in recent years. These composite materials exhibit unique physical and chemical properties and lead them to have great potential applications in the areas of biomedicine, nanotechnology and photonics application [1–4]. Furthermore, the combination of magnetic and fluorescent properties allows the fluorescent particles to be applicable in external magnetic fields [5–7]. These nanocomposites meet the requirements of applications, such as traceability and good dispersibility in a liquid medium.

Among magnetic materials, Fe_3O_4 with special magnetic properties and low toxicity has been widely studied for biological assays, chemical sensors and ferrofluids [8–10]. The design and synthesis of various core–shell architectures based on Fe_3O_4 have been important research subjects in recent years [11–13]. As an important member of the II–VI semiconductor family, zinc sulphide (ZnS) has a room-temperature bandgap. Because of its high refraction index and transmittance in the visible region, ZnS is a well-known phosphor material [14]. Its optical property, superconductivity and ferroelectricity have been extensively investigated in the fields of photoluminescence, electroluminescence and chemical sensing [15–18]. Therefore a combination of Fe_3O_4 and ZnS would contribute to the development and application of magnetic-fluorescent materials. However, because of the lattice mismatch of the components, it is difficult for ZnS to be directly coated on an Fe_3O_4 surface. To solve the problem, we introduced a middle SiO_2 shell and successfully synthesised magnetic-fluorescent Fe_3O_4@SiO_2@ZnS nanocomposites. In this study, the SiO_2 shell protects the magnetic Fe_3O_4 core from oxidation and links ZnS particles to the core. The Fe_3O_4@SiO_2@ZnS nanocomposites were of a bead-like morphology and exhibited excellent magnetic and fluorescence properties. It may serve as a candidate for biomedical applications, such as bioimaging, drug targeting and cell separation.

2. Experimental

2.1. Synthesis of Fe_3O_4 nanoparticles: All reagents were of analytical grade purity and used directly without further purification. Deionised water with resistivity higher than 18 MΩ·cm was used in our experiments. Fe_3O_4 nanoparticles were obtained by means of a solvothermal reaction as reported previously [19], with some modifications. Briefly, $FeCl_3 \cdot 6H_2O$ (1.35 g) and sodium acetate (3.6 g) were dissolved in ethylene glycol (75 ml) under magnetic stirring at room temperature for 30 min. The resulting homogeneous yellow solution was transferred to a Teflon-lined stainless-steel autoclave and sealed to heat at 200°C for 8 h. The precipitated products were washed with deionised water and ethanol three times and then dried in vacuum at 60°C for 12 h.

2.2. Preparation of Fe_3O_4@SiO_2 core–shell nanoparticles: The Fe_3O_4@SiO_2 core–shell nanoparticles were prepared. Briefly, 0.01 g of Fe_3O_4 nanoparticles was treated with 0.1 M HCl aqueous solution (50 ml) by ultrasonication for 30 min. Then, the Fe_3O_4 nanoparticles were collected from the solution with an external magnet and washed with deionised water, and homogeneously dispersed in a mixture of ethanol (80 ml), deionised water (20 ml) and concentrated ammonia aqueous solution (10 ml, 28 wt%), followed by the addition of tetraethyl orthosilicate (TESO, 0.03 g). After being stirring at room temperature for 12 h, the Fe_3O_4@SiO_2 nanoparticles were separated and washed with ethanol and deionised water, and then dried in vacuum at 60°C for 24 h.

2.3. Synthesis of Fe_3O_4@SiO_2@ZnS nanocomposites: The Fe_3O_4@SiO_2@ZnS nanocomposites were synthesised as follows. 0.10 g Fe_3O_4@SiO_2 nanoparticles and 0.75 g zinc acetate were dissolved in 80 ml isopropyl alcohol under stirring. The resulting solution was stirred at room temperature for 12 h. After that, 60 ml of thioacetamide aqueous solution (0.1 M) was added in drops. At the same time, the obtained mixture underwent ultrasonication. After 30 min of ultrasonication, the mixture was transferred to a water bath at 60°C for 8 h under stirring. The product was collected and washed with deionised water and ethanol several times. The prepared sample was dried under vacuum at 60°C for 12 h.

2.4. Characterisation: X-ray diffraction (XRD) patterns of composite microspheres were obtained via a Japan RIGAKU D/max-2400 X-ray diffractometer with Cu/Kα radiation (λ = 0.154056 nm, 40 kV and 200 mA). The morphology was observed using field emission scanning electron microscopy (FESEM, S-4300, Hitachi, Japan) and high-resolution

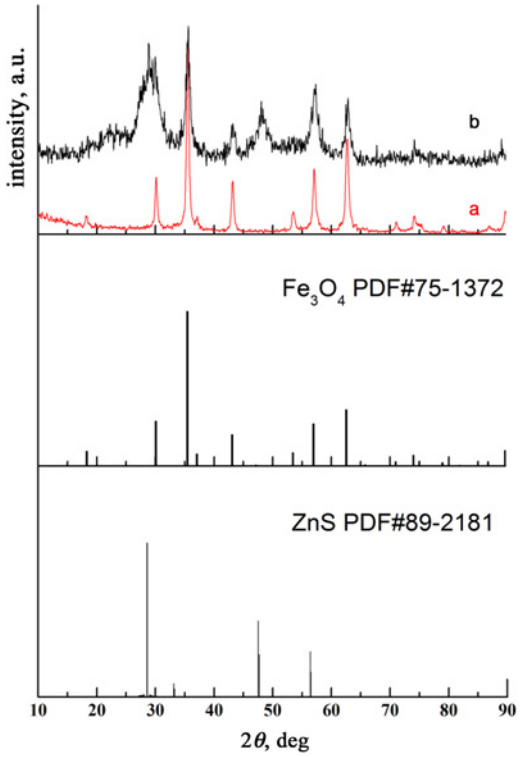

Figure 1 *The XRD patterns of products*

transmission electron microscopy (HRTEM, JEOL IEM-2010, Japan). In addition, the magnetic properties of the composites were characterised by a vibration sample magnetometer (VSM, Lakeshore 7304, America) with an applied field between −15 000 and 15 000 Oe at room temperature. A fluorescence microscope (BX53, AOLYMPUS, Japan) was used to visualise all fluorescent samples.

3. Results and discussion: The crystal structures of the samples were investigated by XRD as shown in Fig. 1. Curve (a) shows the diffraction patterns of as-prepared Fe_3O_4 magnetic particles, which demonstrated the face-centered cubic structure of Fe_3O_4 according to JCPDS Card No. 75-1372. Curve (b) shows the diffraction patterns of Fe_3O_4@SiO_2@ZnS composites. For curve (b), besides the corresponding peaks of Fe_3O_4, all the others were indexed to wurtzite ZnS corresponding to JCPDS Card No. 89-2181. In addition, no obvious SiO_2 peaks were observed, which indicates that the SiO_2 is an amorphous state.

Fig. 2 shows the structural details of the as-prepared Fe_3O_4 nanoparticles and Fe_3O_4@SiO_2@ZnS composites. It can be seen that the well-dispersed Fe_3O_4 particles are of an average size of 200 nm and exhibit microsphere morphology (Fig. 2*a*), while the Fe_3O_4@SiO_2@ZnS composites show needle-like microstructures (Fig. 2*b*). In Fig. 2*c*, a higher magnification SEM image reveals that these needle-like microstructures are built from numerous microspheres. To further identify the size and shape of Fe_3O_4@SiO_2@ZnS composites, HRTEM inspection was conducted as shown in Fig. 2*d*. It can be observed that a great number of microspheres with the size of about 250 nm coalesced

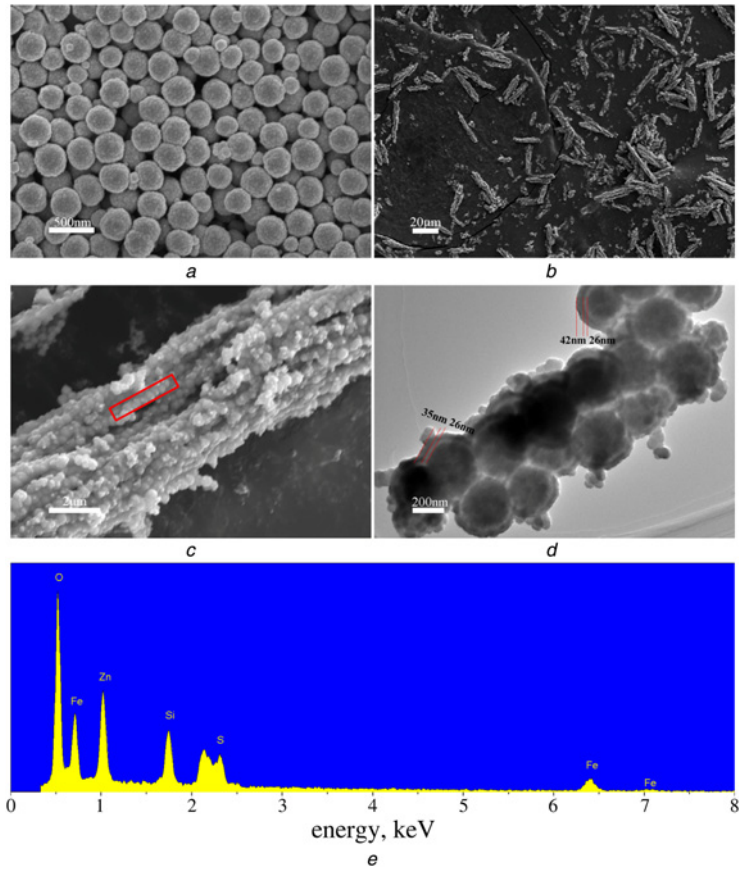

Figure 2 *Structural details*
a FE-SEM image of Fe_3O_4 nanoparticles
b and c FE-SEM image of Fe_3O_4@SiO_2@ZnS nanocomposites
d HR-TEM image of Fe_3O_4@SiO_2@ZnS nanocomposites
e EDX spectrum image of Fe_3O_4@SiO_2@ZnS nanocomposites

doi: 10.1049/mnl.2013.0636

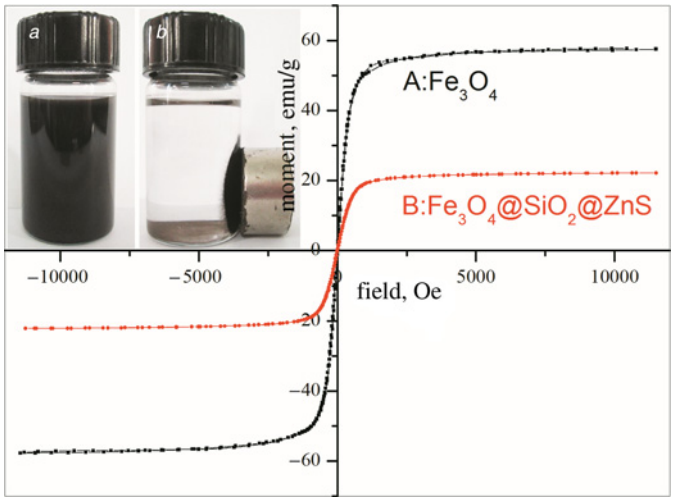

Figure 3 *Magnetic hysteresis curves*
a Magnetic hysteresis curves of Fe_3O_4 nanoparticles
b Fe_3O_4@SiO_2@ZnS nanocomposites at room temperature
Insets are magnetic responsive images of Fe_3O_4@SiO_2@ZnS nanocomposites

together and formed bead-like microstructures, which is in conformity with the FESEM image. Furthermore, it is clearly found that the composites particles are of core–shell structures from the contrast of the HRTEM image, which demonstrates that SiO_2 and ZnS were well coated on the surface of the Fe_3O_4 cores. To identify the composition of the composite materials, we performed an energy dispersive X-ray analysis test on the Fe_3O_4@SiO_2@ZnS sample (Fig. 2*e*). The as-prepared sample is completely composed of Fe, O, Si, Zn and S elements, which further confirms the identification of the Fe_3O_4@SiO_2@ZnS composites.

Magnetic properties were detected at room temperature via a vibrating sample magnetometer. The results show that the saturation magnetisation (M_s) values of Fe_3O_4 particles and Fe_3O_4@SiO_2@ZnS composites were 56.83 emu/g (Fig. 3, curve a) and 22.41 emu/g (Fig. 3, curve b), respectively, which are less than that of the bulk sample of Fe_3O_4 (92 emu/g) [20]. The decrease in the saturation magnetisation of Fe_3O_4@SiO_2@ZnS can be attributed to the SiO_2 shell and ZnS particles. To examine the magnetic response of the composites, the Fe_3O_4@SiO_2@ZnS microspheres were dispersed in the ethanol by sonication or vigorous shaking, resulting in a brown-coloured suspension. The composite materials show fast movement when an external magnetic field is applied (inset in Fig. 3). These results show that Fe_3O_4@SiO_2@ZnS microspheres possess good magnetic responsiveness and redispersibility.

The fluorescence microscope images of Fe_3O_4 and Fe_3O_4@SiO_2@ZnS are shown in Fig. 4. It is found that there is no light emission of pure Fe_3O_4 under UV light irradiation (Fig. 4*a*), while a strong blue light emission can be observed from the Fe_3O_4@SiO_2@ZnS composite materials (Fig. 4*b*).

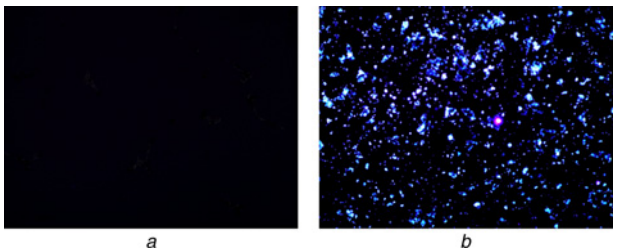

Figure 4 *Images of luminescence*
a Fluorescence microscopy images of pure Fe_3O_4 nanoparticles
b Fluorescence microscopy images of Fe_3O_4@SiO_2@ZnS nanocomposites

4. Conclusions: In summary, novel Fe_3O_4@SiO_2@ZnS composite materials have been prepared using a facile chemical deposition method. The approach of fabrication and the synthetic procedure of nanocomposites is easily reproduced. The morphology of the Fe_3O_4@SiO_2@ZnS composites showed a bead-like structure, which was built from numerous microspheres with an average size of 250 nm. The saturation magnetisation value of the Fe_3O_4@SiO_2@ZnS nanocomposites was 22.41 emu/g. The Fe_3O_4@SiO_2@ZnS microspheres showed good magnetic responsiveness in an external magnetic field and redispersibility in the liquid medium. Furthermore, the nanocomposites can be observed as having a strong blue light emission under UV light irradiation. The combination of magnetic-fluorescent bifunctional properties may lead to Fe_3O_4@SiO_2@ZnS nanocomposites having a variety of potential applications in the field of biomedicine, such as bioimaging, cell separation and drug targeting.

5. Acknowledgments: The authors are grateful for financial aid from the National Natural Science Foundation of China (51262027), the financial support of the Natural Science Foundation of Gansu Province (1104GKCA019; 1010RJZA023), the Science and Technology Tackle Key Problem Item of Gansu Province (2GS064-A52-036-08) and the fund of the State Key Laboratory of Solidification Processing in NWPU (SKLSP201011).

6 References

[1] Mistlberger G., Klimant I.: 'Luminescent magnetic particles: structures, syntheses, multimodal imaging, and analytical applications', *Bioanal. Rev.*, 2010, **2**, pp. 61–101
[2] Zhu Y.F., Fang Y., Kaskel S.: 'Folate-conjugated Fe_3O_4@SiO_2 hollow mesoporous spheres for targeted anticancer drug delivery', *J. Phys. Chem. C*, 2010, **114**, pp. 16382–16388
[3] Di Corato R., Piacenza P., Musaro M., *ET AL.*: 'Magnetic–fluorescent colloidal nanobeads: preparation and exploitation in cell separation experiments', *Macromol. Biosci.*, 2009, **9**, pp. 952–958
[4] Yang P., Zhang A.Y., Cheng X., Zhou G.J., Lü M.K.: 'Morphology-tunable fibers with Fe_3O_4 nanocrystals fabricated through assembly', *J. Colloid Interf. Sci.*, 2010, **351**, pp. 77–82
[5] Kaboudin B., Ghaderian A.: 'A novel magneto-fluorescent microsphere: preparation and characterization of polystyrene-supported Fe_3O_4 and CdS nanoparticles', *Appl. Surf. Sci.*, 2013, **282**, pp. 396–399

[6] Corr S.A., Rakovich Y.P., Gun'ko Y.K.: 'Multifunctional magnetic-fluorescent nanocomposites for biomedical applications', *Nanoscale Res. Lett.*, 2008, **3**, pp. 87–104

[7] Tong L.Z., Liu D.M., Shi J.H., Yang X.W., Yang H.: 'Magnetic and luminescent properties of Fe_3O_4@Y_2O_3:Eu^{3+} nanocomposites', *J. Mater. Sci.*, 2012, **47**, pp. 132–137

[8] Zhu A.P., Yuan L.H., Dai S.: 'Preparation of well-dispersed superparamagnetic iron oxide nanoparticles in aqueous solution with biocompatible N-succinyl-O-carboxymethylchitosan', *J. Phys. Chem. C*, 2008, **112**, pp. 5432–5438

[9] Mohammadi A., Barikani M., Barmar M.: 'Effect of surface modification of Fe_3O_4 nanoparticles on thermal and mechanical properties of magnetic polyurethane elastomer nanocomposites', *J. Mater. Sci.*, 2013, **48**, pp. 7493–7502

[10] Park J.O., Rhee K.Y., Park S.J.: 'Silane treatment of Fe_3O_4 and its effect on the magnetic and wear properties of Fe_3O_4/epoxy nanocomposites', *Appl. Surf. Sci.*, 2010, **256**, pp. 6945–6950

[11] Liu G., Wu H.X., Zheng H.R., *ET AL.*: 'Synthesis and applications of fluorescent-magnetic-bifunctional dansylated Fe_3O_4@ SiO_2 nanoparticles', *J. Mater. Sci.*, 2011, **46**, pp. 5959–5968

[12] Shi H.W., Huang Y., Cheng C., Ji G.Y., Yang Y.X., Yuan H.M.: 'Preparation and characterization of chain-like and peanut-like Fe_3O_4@ SiO_2 core shell structure', *J. Nanosci. Nanotechnol.*, 2013, **13**, pp. 6953–6960

[13] Ma M.L., Zhang Q.Y., Xin T.J., Zhang H.P., Geng W.C., Zhou J.: 'Preparation and characterization of structure-tailored magnetic fluorescent Fe_3O_4/P (GMA–EGDMA–NVCz) core–shell microspheres', *J. Mater. Sci.*, 2013, **48**, pp. 5302–5308

[14] Geng J., Song G.H.: 'One-pot fast synthesis of spherical ZnS/Au nanocomposites and their optical properties', *J. Mater. Sci.*, 2013, **48**, pp. 636–643

[15] Huang Y., Lieber C.M.: 'Integrated nanoscale electronics and optoelectronics: exploring nanoscale science and technology through semiconductor nanowires', *Pure Appl. Chem.*, 2004, **76**, pp. 2051–2068

[16] Borchers C., Stichtenoth D., Müller S., Schwen D., Ronning C.: 'Catalyst–nanostructure interaction and growth of ZnS nanobelts', *Nanotechnology*, 2006, **17**, pp. 1067–1071

[17] Kim M.R., Kang Y.M., Jang D.J.: 'Synthesis and characterization of highly luminescent CdS@ZnS core-shell nanorods', *J. Phys. Chem. C*, 2007, **111**, pp. 18507–18511

[18] Issac A., Jin S.Y., Lian T.Q.: 'Intermittent electron transfer activity from single CdSe/ZnS quantum dots', *J. Am. Chem. Soc.*, 2008, **130**, pp. 11280–11281

[19] Xuan S.H., Wang Y.-X.J., Yu J.C., Leung K.C.-F.: 'Preparation, characterization, and catalytic activity of core/shell Fe_3O_4@ polyaniline@Au nanocomposites', *Langmuir*, 2009, **25**, pp. 11835–11843

[20] Liu J.H., Wei J., Li S.M.: 'Preparation and characteristics of Fe_3O_4 magnetic thin films plated on hollow glass spheres', *Mater. Lett.*, 2007, **61**, pp. 1529–1532